Vol. 38 No. 3 Journal of the Communications Research Laboratory November 1991
Printed in Tokyo, Japan pp. 577 – 604

IV. EXPERIMENTAL RESULTS

IV.6 INTERNATIONAL VLBI EXPERIMENT USING THE WAVE-FRONT CLOCK TECHNIQUE

By
Hitoshi KIUCHI, Tetsuro KONDO, and Josef POPELAR*

(Received on March 18, 1991)

ABSTRACT

A prototype wavefront clock system has been developed for application to the Mark-III and K-3 VLBI systems. In this system, the reference clock used for both the frontend and backend of the VLBI data acquisition terminal is controlled directly according to a calculated a priori delay rate. By using this wavefront clock system in a VLBI experiment, fringe stopping can be simultaneously applied to all received frequencies to aid in cross correlation processing. This report discusses the performance of this wavefront clock system and the results of some fundamental experiments.

1. Introduction

Very Long Baseline Interferometry (VLBI)[1]–[3] is a measurement technique in which the baseline vector between two stations is measured by observing the different arrival time of radio waves radiated from quasars. It is necessary in VLBI, however, to calibrate the Doppler frequency caused by the earth rotation at signal processing. The Doppler shift has usually been compensated for during the correlation processing in a VLBI experiment. It is possible, though, to compensate for the Doppler shift when signals are received at each station in a method called the "wavefront clock" technique. Consequently, the correlation processing of data acquired by means of the wavefront clock technique can be easier than the current processing method. In this report, we discuss a wavefront clock method for conventional Mark-III and K-3 VLBI systems. A significant characteristic of this method is that the wavefront clock system controls the reference signals directly. We also investigate the application of this technique to both a short domestic baseline and a long international baseline between Kashima and Algonquin in Canada. This second experiment is significant because of the large Doppler influence on east-west baselines like the Japan-Canada one. In future experiments, much of the Doppler shift in space VLBI will be able to be removed for baselines longer than the earth's diameter.

2. Principle of the Wavefront Clock Technique

Let us suppose that a observer is watching a wave moving on the water. This wave can be expressed as a function of time and its height. In particular, if the height of the wave is sampled every

*Energy, Mines and Resources Canada.

so many units in time, then time can be denoted on the horizontal axes and the wave's height on the vertical axes. The height of the wave is unique to a particular point in time. In other words, the wave has time notches (code), and such a time notch on the wave is called a "wavefront clock".

First, let's assume that an observer watching a wave is sitting in a stopped boat, and a clock on the boat and the wavefront clock on the wave had time notches of equal spacing. The detected wave would then appear like that in Fig. 1A.

Secondly, let's assume that the boat is now moving towards the wave. The notches on the wave would now be different from that of the boat since the velocity of the wave is constant. The notch period of the wave would appear shorter than that of the boat. This is the Doppler shift. The observed in wave Fig. 1B is different but similar to that in Fig. 1A.

Lastly, if the observer used the notch on the wave (the wavefront clock) as his own clock, the observed wave shown in Fig. 1C would be the same as that in Fig. 1A. However, the clock on the wave

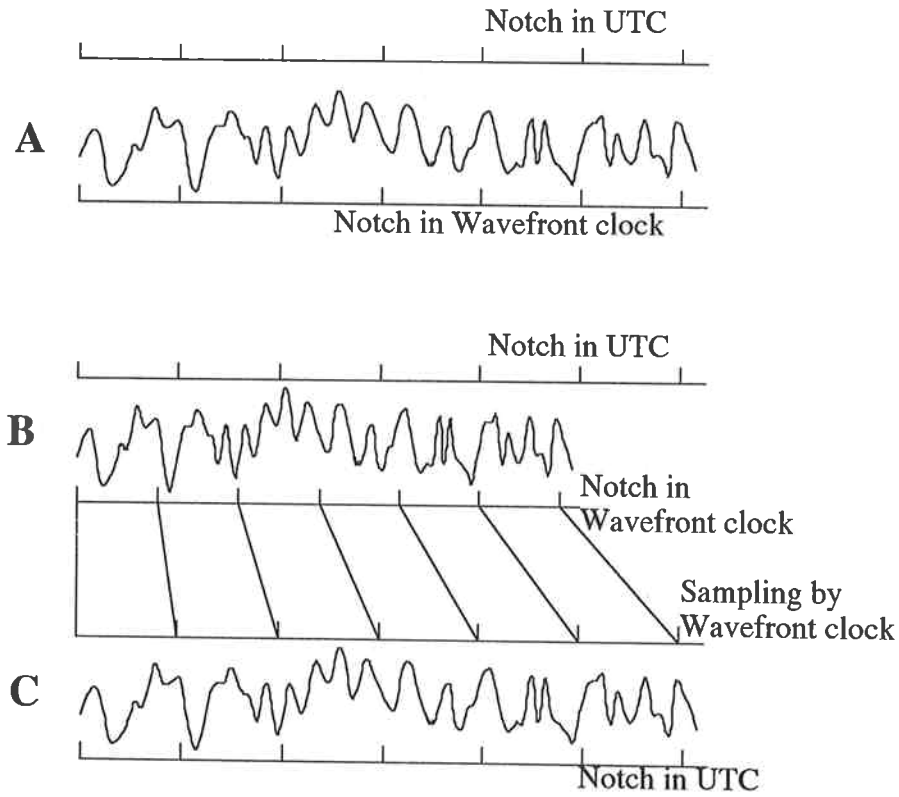

A: Detected signal with Non-Doppler shift
B: Detected signal with Doppler shift
C: After sampling signal using Wavefront clock
UTC: Universal time coordinates

Fig. 1 Concept of a wavefront clock.

is ahead of that on the boat, which means that the observer on the moving boat could observe a wave before an observer in a stopped boat back at the first boat's starting point. The Doppler shift influences both the frequency domain and time domain. After all, using the wavefront clock (time on the wave) instead of the clock on the boat, one can offset the Doppler shift caused by the moving boat.

It is possible to apply this theory to radio waves received from quasars. In VLBI observation, each observed station is moving with different speed against the radio wave due to the rotation of the earth. If we use the same clock rate such as universal time coordinates (UTC) at both stations, the observed signals include the Doppler effect cause by the earth rotation. It is impossible to obtain a "fringe," an interference pattern between two signals, without Doppler cancelling using some method. In conventional VLBI, cancelling of the Doppler shift is done after data acquisition, at the correlation processing site. However, if a wavefront clock was used, cancelling of the Doppler shift could be done during data acquisition at each observed station. In order to do this efficiently, the geocenter of the earth is adopted as a reference point. This choice is a matter of convenience since it greatly simplifies the geometry of the array. The time reference is selected to be a UTC clock located at the geocenter. All corrections are then made with respect to this reference point instead of relative to another antenna. Consequently, the wavefront clock signal (rate and offset) must be determined from the UTC clock. The earth is a sphere, and stations located at different sites will generally not observe the wavefront at the same time. In addition, the rotation of the earth will cause the signals arriving at each antenna to be Doppler shifted, the amount of which will vary with station location. The wavefront clock at each station will have a different clock rate and clock offset depending on station position and star position.

2.1 The VLBI Observation Equation[4]–[7]

We consider the correlation processing between observed data of station X and that of station Y (Fig. 2). Let $x(t)$ be the received signal at X station and $y(t)$ be the received signal at Y station expressed in UTC. Suppose that a signal from a quasar is received at station Y some time delay τ_g after being received at station X. The relationship between $x(t)$ and $y(t)$ is expressed as

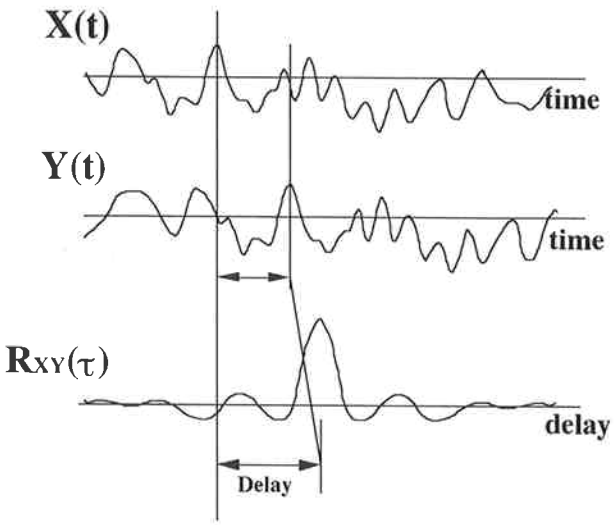

Fig. 2 Correlation function.

$$y(t) = x\left(t - \tau_g\right). \qquad (1)$$

The Fourier Transform of $y(t)$ is

$$\begin{aligned} Y(\omega) &= \int y(t) e^{-j\omega t} dt \\ &= X(\omega) e^{-j\omega\tau_g}, \end{aligned} \qquad (2)$$

where ω is angular frequency of the received signal.

It is assumed that the local frequency of the X station is described as ω_x, its phase as ϕ_x, the local frequency of the Y station as ω_y, and its phase as ϕ_y. The video signal in the upper sideband can then be expressed as

$$X(\omega) = X\left(\omega + \omega_x\right)\exp\left(-j\phi_x\right) \quad \omega > 0$$

$$Y(\omega) = Y\left(\omega + \omega_y\right)\exp\left(-j\phi_y\right) \quad \omega > 0. \qquad (3)$$

The cross-spectrum function $S'_{xy}(\omega)$ can be written as

$$\begin{aligned} S'_{xy}(\omega) &= X(\omega) Y^*(\omega) \\ &= X\left(\omega + \omega_x\right)\exp\left(-j\phi_x\right) \; Y^*\left(\omega + \omega_y\right)\exp\left(+j\phi_y\right), \end{aligned} \qquad (4)$$

where * indicates complex conjugate. In addition, $\omega + \omega_y$ can be expressed as

$$\omega + \omega_y = \left(\omega + \omega_x\right) + \left(\omega_y - \omega_x\right). \qquad (5)$$

By substituting Eq. (2) and Eq. (5) into Eq. (4), we get

$$\begin{aligned} &S'_{xy}(\omega) \\ &= X\left(\omega + \omega_x\right)\exp\left(-j\phi_x\right)\left\{X^*\left(\omega + \omega_x\right)\exp\left(j\left(\omega + \omega_x\right)\tau_g\right)\right\}\exp\left(j\left(\omega_y - \omega_x\right)t\right)\exp\left(+j\phi_y\right) \\ &= S_{xx}\left(\omega + \omega_x\right)\exp\left[j\left\{\phi_y - \phi_x + \left(\omega_y - \omega_x\right)t\right\}\right]\exp\left(j\left(\omega + \omega_x\right)\tau_g\right) \\ &= S_{xx}(\omega')\exp(j\theta)\left\{\exp\left(j\omega\tau_g\right)\exp\left(j\omega_o\tau_g\right)\right\} \end{aligned} \qquad (6)$$

where $\theta = (\phi_y - \phi_x) + (\omega_y - \omega_x)t$: local oscillator phase difference;
$\omega' = \omega + \omega_x$: radio frequency;
$\omega_o = \omega_x$: local oscillator frequency.

If the total of time synchronization error, instrumental delay and propagation delay are expressed as τ_e, then $S'_{xy}(\omega)$ can be rewritten as follows:

$$S'_{xy}(\omega) = S'_{xy}(\omega)\exp(j\omega\tau_e)\exp(j\omega_o\tau_e).$$

The cross correlation function $R_{xy}(\tau)$ is the Fourier transform of $S'_{xy}(\omega)$, as follows;

$$\begin{aligned} &R_{xy}(\tau) \\ &= \int_{-\infty}^{+\infty} S_{xx}(\omega')\exp(\pm j\theta)\left\{\exp\left(\pm j\omega_o\left(\tau_g+\tau_e\right)\right)\exp\left(j\omega\left(\tau_g+\tau_e\right)\right)\right\}\exp(j\omega\tau)d\omega/2\pi \end{aligned} \quad \ldots (7)$$

where $+$: in case of upper side band $\omega > 0$
$-$: in case of lower side band $\omega < 0$
τ: time lag

$$\begin{aligned} &= \left[\cos\left\{\theta+\omega_o\left(\tau_g+\tau_e\right)\right\} - j\sin\left\{\theta+\omega_o\left(\tau_g+\tau_e\right)\right\}\right]\int_{-\infty}^{0} S_{xx}(\omega')\exp\left\{j\omega\left(\tau+\tau_g+\tau_e\right)\right\}d\omega/2\pi \\ &+ \left[\cos\left\{\theta+\omega_o\left(\tau_g+\tau_e\right)\right\} + j\sin\left\{\theta+\omega_o\left(\tau_g+\tau_e\right)\right\}\right]\int_{0}^{+\infty} S_{xx}(\omega')\exp\left\{j\omega\left(\tau+\tau_g+\tau_e\right)\right\}d\omega/2\pi \\ &= 2\cos\left\{\theta+\omega_o\left(\tau_g+\tau_e\right)\right\}\int_{0}^{+\infty} S_{xx}(\omega')\cos\left\{\omega\left(\tau+\tau_g+\tau_e\right)\right\}d\omega/2\pi \\ &- 2\sin\left\{\theta+\omega_o\left(\tau_g+\tau_e\right)\right\}\int_{0}^{+\infty} S_{xx}(\omega')\sin\left\{\omega\left(\tau+\tau_g+\tau_e\right)\right\}d\omega/2\pi. \end{aligned} \quad \ldots\ldots\ldots (8)$$

If the received signal were white noise and the bandwidth indicated by B[Hz], then

$$\begin{aligned} S_{xx}(\omega') = 1 &: \quad 0 \le \omega' \le 2\pi B \\ 0 &: \quad \text{other.} \end{aligned}$$

Equation (8) can then be rewritten as

$$\begin{aligned} &R_{xy}(\tau) \\ &= 2\cos\left\{\theta+\omega_o\left(\tau_g+\tau_e\right)\right\}\int_{0}^{2\pi B}\cos\left\{\omega\left(\tau+\tau_g+\tau_e\right)\right\}d\omega/2\pi \\ &-2\sin\left\{\theta+\omega_o\left(\tau_g+\tau_e\right)\right\}\int_{0}^{2\pi B}\sin\left\{\omega\left(\tau+\tau_g+\tau_e\right)\right\}d\omega/2\pi \end{aligned} \quad \ldots\ldots\ldots\ldots\ldots (9)$$

$$= 2\cos\left\{\theta + \omega_o\left(\tau_g + \tau_e\right)\right\}\frac{1}{2\pi\left(\tau + \tau_g + \tau_e\right)}\sin 2\pi B\left(\tau + \tau_g + \tau_e\right)$$

$$+2\sin\left\{\theta + \omega_o\left(\tau_g + \tau_e\right)\right\}\frac{1}{2\pi\left(\tau + \tau_g + \tau_e\right)}\left\{\cos 2\pi B\left(\tau + \tau_g + \tau_e\right) - 1\right\}$$

$$= 2B\left[\frac{\sin \pi B\left(\tau + \tau_g + \tau_e\right)}{\pi B\left(\tau + \tau_g + \tau_e\right)}\right]\cos\left\{\theta + \omega_o\left(\tau_g + \tau_e\right) + \pi B\left(\tau + \tau_g + \tau_e\right)\right\}. \quad \ldots\ldots\ldots\ldots (10)$$

In VLBI, radio emissions from a radio source several billion light years away is often received by two stations. As the received radio wave is very weak, it is necessary to integrate a very large amount of data and $R_{xy}(\tau)$ has to be kept to a fixed value in phase during signal integration. In Eq. (10), the term $2B[\{\sin\pi B(\tau+\tau_g+\tau_e)\}/\pi B(\tau+\tau_g+\tau_e)]$ provides the function's envelope with the shape of $\sin(x)/x$. It is impossible to obtain a fringe without keeping the phase of the cosine function in Eq. (10) constant.

If no frequency conversion with signal receiving and direct data correlation with radio frequencies were conducted, then Eq. (10) could be rewritten as Eq. (11) below, since ϕ_y, ϕ_x, ω_y, and ω_x are zero in Eq. (3) to Eq. (10).

$$R_{xy}(\tau) = 2B\frac{\sin \pi B\left(\tau + \tau_g + \tau_e\right)}{\pi B\left(\tau + \tau_g + \tau_e\right)}\cos\left\{\pi B\left(\tau + \tau_g + \tau_e\right)\right\}. \quad \ldots\ldots\ldots\ldots (11)$$

In order to obtain a fringe, the term $\{\pi B(\tau + \tau_g + \tau_e)\}$ must be kept constant, so that

$$d\tau / dt = -d\left(\tau_g + \tau_e\right)/dt. \quad \ldots\ldots\ldots\ldots (12)$$

This equation means that the rate of change in $(\tau_g + \tau_e)$ can be canceled by that of τ in a process called "delay tracking". Delay tracking is realized by adding the delay to acquired data or by controlling the clock rate. Equations (11) and (12) indicate that if correlation processing was performed with radio frequencies directly, then a fringe could be obtained without "fringe rotation", which is explained in the following.

In general, however, the radio frequency signal is heterodyne converted (with a down converter) to intermediate frequency or video frequency, as described by Eq. (3), and we must use Eq. (10). In order to keep $\{\theta + \omega_o(\tau_g + \tau_e) + \pi B(\tau + \tau_g + \tau_e)\}$ constant, the rate of change of the terms in these brackets must be zero, and the third term here should become

$$d\tau/dt = -d(\tau_g + \tau_e)/dt.$$

This equation is the same as Eq. (12), the delay tracking. In addition, the second term of the cosine function in Eq. (10) can be canceled by θ, so that

$$d\theta/dt = -d\{\omega_o(\tau_g + \tau_e)\}/dt$$

where $\theta = (\phi_y - \phi_x) + (\omega_y - \omega_x)t$ is the local oscillator phase difference (see Eq. (6)) and

$$\left(\omega_y - \omega_x\right) = -d\left\{\omega_o\left(\tau_g + \tau_e\right)\right\} / dt. \qquad \ldots\ldots\ldots\ldots\ldots\ldots\ldots\ldots\ldots\ldots (13)$$

The effect expressed by Eq. (13) is called "fringe (lobe) rotation". Fringe rotation is performed by adding the phase to acquired data or by controlling the clock rate.

3. VLBI Methods

There are several methods for executing delay tracking and fringe rotation to cancel the Doppler shift, as follows:

i) Conventional VLBI method
ii) Canadian VLBI wavefront clock method
iii) Kashima's VLBI wavefront clock method.

We discuss these methods in this section.

3.1 Conventional VLBI system[5]–[10]

In this system, all frequencies are phase-locked to the fixed reference frequency from the hydrogen maser and the acquired data includes the Doppler shift caused by earth rotation. The fringe rotation and delay tracking are performed in the correlation processor at the correlation site, as shown in Fig. 3. In order to cancel the Doppler frequency, the fringe frequency (Eq. (13)) is multiplied to Eq. (7), and delay tracking is performed by bit shifting. Here, bit shifting is the same as controlling the sampling clock. In this method, it is easy to incorporate fully digital circuits.

Two kinds of loss accompany correlation processing in conventional VLBI: fringe rotation compensation and fractional bit correction. Fringe rotation is compensated by multiplying the cross-correlation function by $\exp(j\omega_f t)$, where ω_f is frequency of the fringe rotation (Eq. (13)). The function $\exp(j\omega_f t)$ can be approximated with the three-level functions (1, 0 and –1), shown in Fig. 4. In particular, $\exp(j\omega_f t)$ can be expressed as $C(t) + jS(t)$ in a Fourier series:

$$C(t) + jS(t) = \sum_{m=0}^{\infty} \gamma_m \exp\left[j(-1)^m (2m+1)\omega_f t\right] \qquad \ldots\ldots\ldots\ldots\ldots\ldots (14)$$

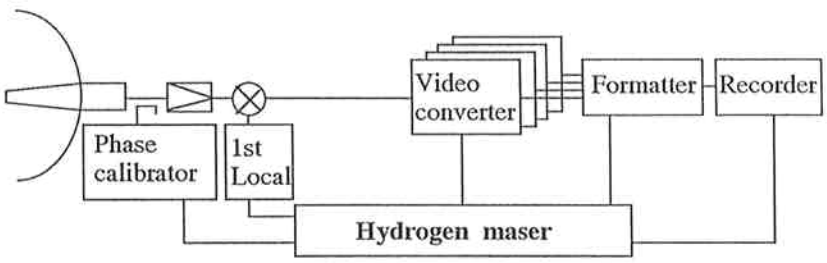

Fig. 3 Conventional VLBI system.

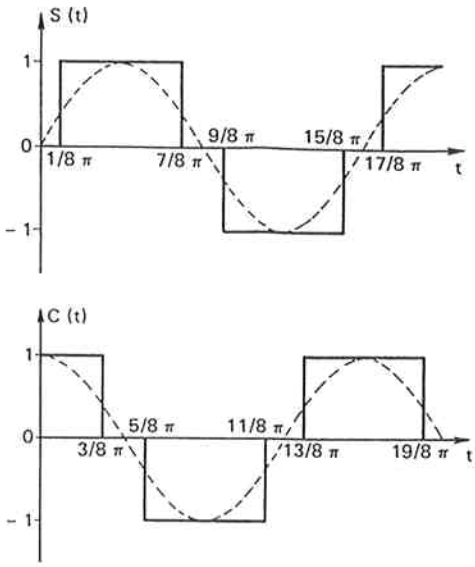

Fig. 4 Three-level approximation.

where

$$\gamma_m = \frac{4}{\pi}\frac{1}{2m+1}\cos\frac{(2m+1)\pi}{8}. \quad \ldots\ldots\ldots\ldots\ldots\ldots\ldots\ldots\ldots\ldots (15)$$

Only the first term of the series to compensates the fringe rotation, and the others are dispersed in correlated power. Coherence loss β_{fr} is estimated by the ratio of the first term, γ_o, to the root sum squares of all terms.

$$\beta_{fr} = \frac{\gamma_o}{\sqrt{\sum|\gamma_m|^2}}. \quad \ldots\ldots\ldots\ldots\ldots\ldots\ldots\ldots\ldots\ldots\ldots\ldots\ldots\ldots (16)$$

Substituting Eq. (15) into Eq. (16), we get

$$\beta_{fr} = \frac{2}{3}\frac{4}{\pi}\cos\frac{\pi}{8} = 0.960. \quad \ldots\ldots\ldots\ldots\ldots\ldots\ldots\ldots\ldots\ldots\ldots\ldots\ldots\ldots (17)$$

The estimated coherence loss of the three-level approximation is 4%.

Another coherence loss is discontinuous delay tracking performed by bit shifting in a correlator buffer memory, in which the loss is due to fractional bits. Illustrated by the solid lines in Fig. 5, which shows the delay versus time in baseband frequency, the simplest way to delay tracking is to shift one

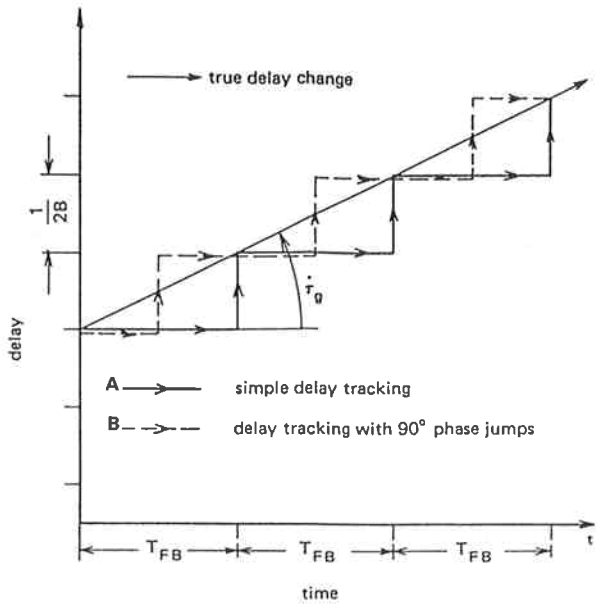

Fig. 5 A: Delay tracking (bit shift only), B: Delay tracking (one bit shift with 90-deg. jump).

bit of data after the delay change corresponding to the one bit has occurred. In this case, the coherence loss is expressed as

$$\beta_{fb} = \frac{1}{B} T_{fb} \int_0^B \int_0^{T_{fb}} \cos\left[2\pi (f - B/2) \frac{d\tau_g}{dt} t \right] dt \; df, \qquad \ldots\ldots\ldots\ldots\ldots\ldots (18)$$

where B is video bandwidth in Hz and T_{fb} is the time required for the change in delay by one bit, expressed as

$$T_{fb} = \frac{1}{2B \dfrac{d\tau_g}{dt}}. \qquad \ldots\ldots\ldots\ldots\ldots\ldots\ldots\ldots\ldots\ldots\ldots\ldots\ldots\ldots (19)$$

Substituting Eq. (19) into Eq. (18), the calculated coherence is $\beta_{fb} = 0.87$. The estimated coherence loss is 13%. In conventional VLBI, in order to reduce coherence loss, the delay tracking method shown in Fig. 5 by dashed lines is adopted. Case (a) applies when the fringe rotator corrects the phase for zero-baseband frequency, and case (b) applies when the fringe rotator also inserts a $\pi/2$ phase shift when the delay changes by one Nyquist sample. Figs. 6a and 6b shows the phase across the baseband at three and five different times. Case (b) consists of a 90-degree phase jump and bit shift carried out simultaneously. This method is as effective as fringe stopping at the center of the video

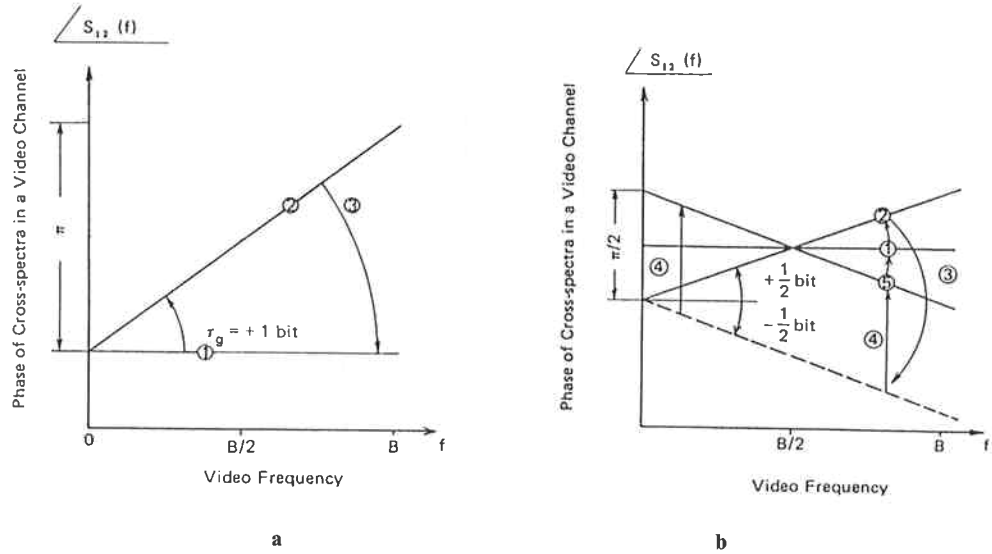

Fig. 6 a: The phase across the baseband (bit shift only), b: The phase across the baseband (one bit shift with 90-deg. jump).

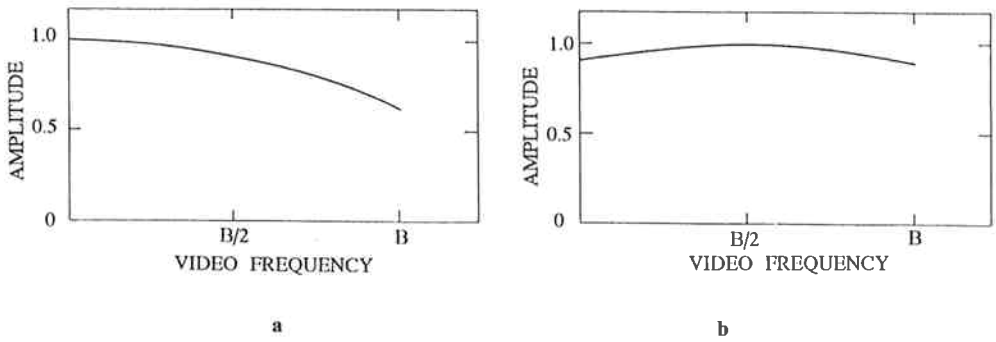

Fig. 7 a: Average amplitude across the baseband (bit shift only), b: Average amplitude across the baseband (one bit shift with 90-deg. jump).

(baseband) frequency. Figs. 7a and 7b shows the average amplitude across the baseband for the above two cases. The coherence loss of case (b) can be estimated by the following equation:

$$\beta_{fb} = \frac{1}{B} T_{fb} \int_0^B \int_0^{T_{fb}} \cos\left[\pi (f - B/2) \frac{d\tau_g}{dt} t \right] dt \; df. \qquad \ldots\ldots\ldots\ldots\ldots\ldots (20)$$

The estimated coherence is 0.966, and the coherence loss is 3.4%.

3.2 Canadian Wavefront Clock System[11][12]

This system differs from conventional VLBI systems in that fringe rotation and delay corrections are performed at the observed station instead of at the correlation stage. In current VLBI, the corrections are made during playback on each baseline and the data correlated. It is clear, though, that if the array consists of a large number of telescopes, corrections must be made over a very large number of baselines. The correlation system can then become complicated and costly since it is desirable to do the corrections and correlation over all the baselines at once.

The block diagram for the Canadian VLBI wavefront clock system is shown in Fig. 8. This system uses a fixed 1st local frequency and a phase calibration signal as in the conventional VLBI system. But the estimated phase, which is calculated at radio frequency equivalent to the center of video frequency is added during signal conversion in each video converter. Only a wavefront clock is used as a sampling clock. A fringe rotation using the Canadian wavefront clock is equivalent to changing "θ" to "θ + additional phase" in Eq. (6) to Eq. (10), when the additional phase is calculated by Eq. (13).

This system can be composed of digital circuits as in conventional VLBI systems. The four-phase clock is used for fractional bit-shift correction, the same as case (b) in Figs. 5, 6, and 7 of the previous section. However, coherence loss, as discussed in the previous section, must be considered. The local oscillator (for the video converter) and the 1-bit sampler are controlled by the wavefront clock whose epoch is set equal to the time a given wavefront arrives at the geocenter.

Since the additional phase is dependent on RF frequency, it is different for each channel. It is impossible to calibrate the Doppler shift of the upper sideband and that of the lower sideband simultaneously. The additional phase is, of course, added to the phase calibration signal. The Canadian

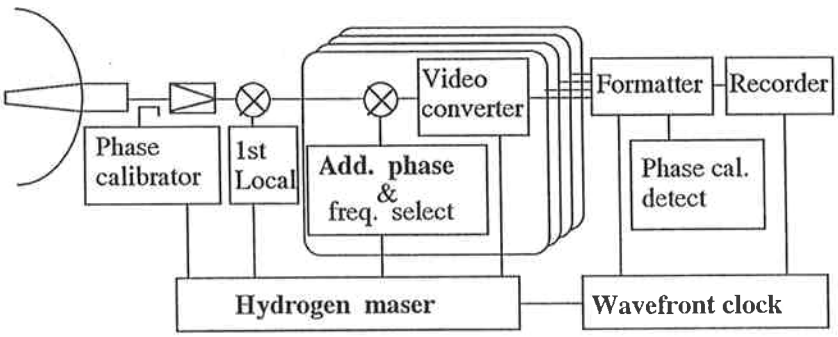

Fig. 8 Canadian VLBI system.

VLBI system has to re-cancel this additional phase in the phase calibration signal. After re-canceling, the phase calibration signal is detected. The delay tracking is performed by using the wavefront clock on sampling simultaneously.

3.3 Kashima's Wavefront Clock System (KWFC)

This system uses the wavefront clock for signal frequency conversion, sampling and the phase calibration signal, so that all of the station's reference signals are phase locked to the wavefront clock. The wavefront clock system controls the reference signals directly, and the setting resolution of the frequency is 7×10^{-13}. A block diagram of this system is shown in Fig. 9. A fringe rotation using Kashima's wavefront clock (KWFC) is equivalent to changing "$(\omega_y - \omega_x)$" to "$(\omega_y - \omega_x)$ + fringe frequency" in UTC coordinates in Eq. (6) to Eq. (10). However, it is also possible to describe the fringe rotation by changing "$(\omega_y - \omega_x)$ of UTC coordinate" to "$(\omega_y - \omega_x)$ of wavefront clock coordinate", which is much simpler. This system can be applied to conventional VLBI systems without modification, and to any frequency type of VLBI experiments, since $d\tau/dt$ is equivalent in all frequencies, or in other words, $d\tau/dt$ is independent of frequency (the fringe frequency is calculated by $\omega d\tau/dt$, Eq. (13)). The fringe rotation is performed for all frequencies together so that it is not necessary to cancel the Doppler shift in each channel. Furthermore, Eqs. (7), (8), (9), and (10) show that it is possible for KWFC to cancel the fringe rotation for both USB and LSB simultaneously. This is impossible in conventional VLBI and Canadian VLBI, since the rotation of fringe phase is different in both sidebands and in different frequencies due to the use of a fixed 1st local.

The phase of each station signal is closed, that is, using the wavefront clock the phase calibration signal is detected at 10 kHz in each station. Of course, it is not measured to 10 kHz in UTC coordinates but in wavefront clock coordinates. We will discuss the phase calibration signal in more detail in Subsection 3.3.1.

Next, we discuss the delay tracking and fringe rotation of the KWFC VLBI system. Letting β be ω_y/ω_x, then Eq. (13) becomes

$$\omega_x(1-\beta) = d\left\{\omega_o\left(\tau_g + \tau_e\right)\right\} / dt. \qquad \ldots\ldots\ldots\ldots\ldots\ldots\ldots\ldots\ldots\ldots (21)$$

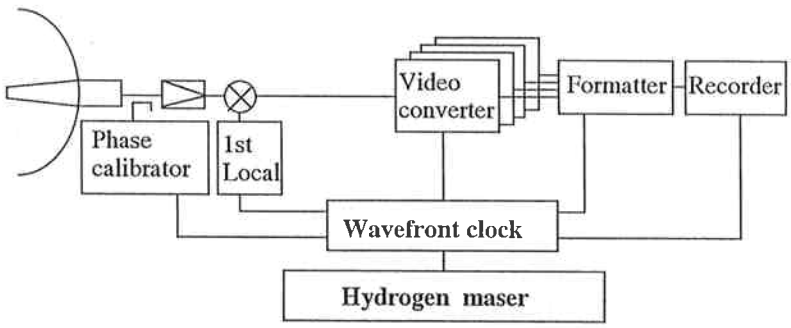

Fig. 9 Kashima's VLBI system.

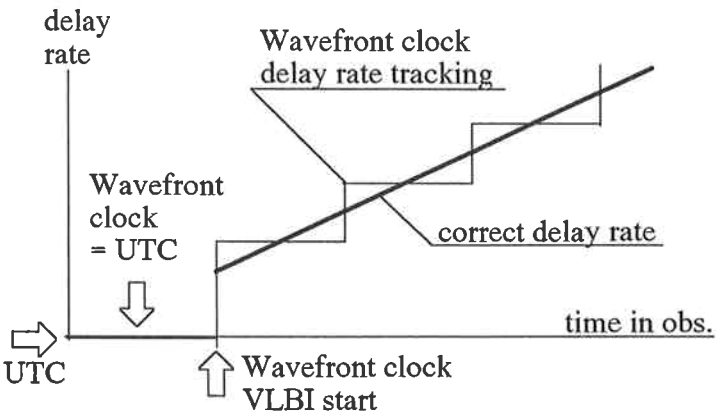

Fig. 10 Wavefront clock delay tracking.

This equation indicates the fringe rotation, which is in the same form as the Doppler shift. In conventional VLBI systems, the differentiated frequency $\omega_x(1-\beta) = d\{\omega_o(\tau_g + \tau_e)\}/dt$ is added to the acquired data of station Y in correlation processing for cancelling the Doppler shift. In the wavefront clock VLBI system, the differentiated frequency $\omega_x(1-\beta) = d\{\omega_o(\tau_g + \tau_e)\}/dt$ is added to the local frequency of station Y during data acquisition for cancelling the Doppler shift. Multiplying the 1st local frequency by $(1-\beta)$ is equivalent to multiplying the reference frequency by $(1-\beta)$. If we choose to multiply the reference frequency by $(1-\beta)$, fringe rotation and delay tracking can be carried out simultaneously, because they have identical terms in Eqs. (12), (13) and (21). This is the fundamental idea behind KWFC. The delay tracking is shown in Fig. 10; the plot shows the delay rate versus time at baseband frequency.

The geocenter of the Earth is adopted as a reference point. The time reference is selected to be a UTC clock located at the geocenter. All corrections are then made with respect to this reference point instead of relative to another antenna. Since fringe rotation is done at the base station, correlation processing can be performed over all the baselines at once.

3.3.1 Phase calibration in the KWFC method[13]

It is possible to describe the phase of a reference signal in the wavefront clock system in UTC coordinates as follows (see Eq. (21)):

$$\omega_L = (1+\alpha)\omega_{ref}, \qquad \cdots\cdots\cdots\cdots\cdots\cdots\cdots\cdots\cdots\cdots\cdots\cdots\cdots\cdots\cdots\cdots (22)$$

where ω_L is the wavefront clock output signal;
ω_{ref} is the fixed reference signal from the hydrogen maser.

The observer uses ω_L as if it was a reference signal from a hydrogen maser. A drive signal of the comb generator (Fig. 11) is expressed as

$$\Phi_1(t) = \omega_L(t - \tau_{\text{cable}}), \qquad \cdots\cdots\cdots\cdots\cdots\cdots\cdots\cdots\cdots\cdots\cdots\cdots\cdots\cdots\cdots\cdots (23)$$

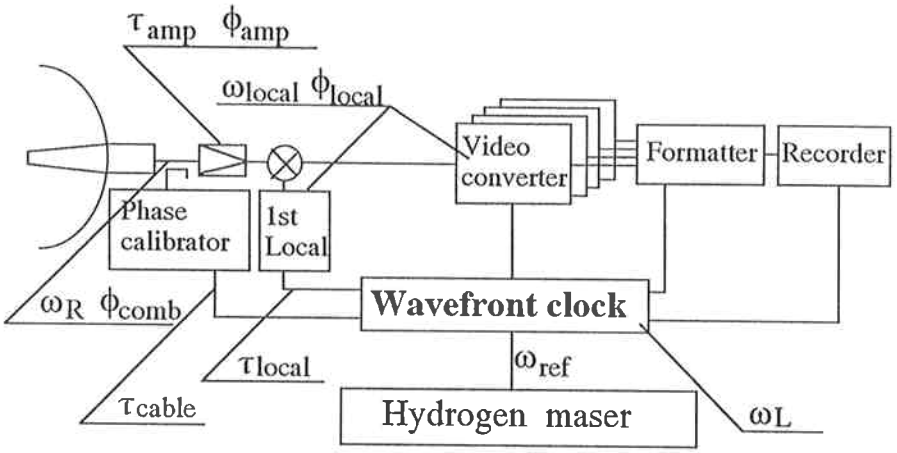

Fig. 11 Phase calibration signal.

where τ_{cable} is propagation delay of the cable.

The output signal (comb signal) is expressed as

$$\begin{aligned}\Phi_2 &= n\Phi_1 + \Phi_{\text{comb}} \\ &= \omega_R\left(t-\tau_{\text{cable}}\right)+\Phi_{\text{comb}},\end{aligned} \qquad \cdots\cdots\cdots\cdots\cdots\cdots\cdots\cdots\cdots\cdots (24)$$

where $\omega_R = n\omega_L$, n: integer (multiplexed number);
Φ_{comb} is supplement phase by the comb generator.

The output signal of the video converter Φ_{vc} is

$$\Phi_{vc} = \omega_R\left(t-\tau_{\text{cable}}\right)+\Phi_{\text{comb}}-\omega_R\tau_{\text{amp}}-\Phi_{\text{amp}}-\omega_{\text{local}}\left(t-\tau_{\text{local}}\right)-\Phi_{\text{local}} \qquad \cdots (25)$$

where $\omega_{\text{local}} = m\omega_L$: total local frequency for heterodyne conversion;
m is not necessarily a integer;
τ_{amp} is delay of amplifier;
Φ_{amp} is supplement phase by amplifier;
Φ_{local} is supplement phase by frequency conversion;
τ_{local} is delay by transmitted cable.

This signal is delayed the same as the received signal (which includes the Doppler frequency). Frequency is differentiated by phase. The detected frequency is thus:

$$\frac{1}{2\pi}\frac{d\Phi_{vc}}{dt} = \frac{1}{2\pi}\left(\omega_R - \omega_{\text{local}}\right)$$
$$= \left[\frac{1}{2\pi}(1+\alpha)\omega_{\text{ref}}\right](n-m). \quad \ldots\ldots\ldots\ldots\ldots\ldots\ldots\ldots\ldots\ldots (26)$$

The first term in brackets on the right-hand side of Eq. (26) represents the reference frequency of the wavefront clock, the same as Eq. (22). The detected frequency is the reference frequency multiplied by (n-m). If the right-hand side of Eq. (26) is selected as 10 kHz, the detected frequency is always 10 kHz in wavefront clock coordinates. The phase calibration signal is always detected as 10 kHz in spite of using the wavefront clock. The wavefront clock is similar to a conventional VLBI clock whose reference has a staggered clock rate.

4. Development of the Wavefront Clock

In our wavefront clock system, the rate of the reference clock used for both the frontend and backend of the VLBI data acquisition terminal is controlled directly according to a calculated a priori delay rate. This wavefront Clock method can be implemented even in conventional VLBI systems without modification. The development of our wavefront clock system included preparation of:

1) Hardware for reference frequency control
2) Software for a priori value calculation.

Next, in order to check system performance, we carried out four kinds of experiments step by step as follows:

1) Zero baseline experiment for checking the system
2) Short (domestic) baseline experiment for detecting the fringes
3) Intermediate (domestic) baseline experiment for checking bandwidth synthesizing capability to obtain a precise delay time
4) Long (international) baseline experiment between Japan and Canada for checking the total system feasibility.

4.1 Hardware

In addition to direct control of the reference signal, frequency resolution and signal clarity are important factors in our wavefront clock system. In this regard, we have constructed two types of wavefront clock system, as follows.

4.1.1 Direct control of the hydrogen maser's output signal

This is the optimum method for maintaining frequency stability. It is, however, necessary to improve the electronics of the hydrogen maser, and this makes it difficult to apply to any other station. This improvement is necessary since the output signal of the maser physics package is fixed at 1.420405752 GHz and not controlled even if the hydrogen maser is used for a wavefront clock. Output frequency from the electronics package of the hydrogen maser, however, is controlled by computer, as shown in Fig. 12a. With this method, frequency control is very accurate and frequency resolution reaches 7×10^{-13} with a mili-Hertz resolution synthesizer.

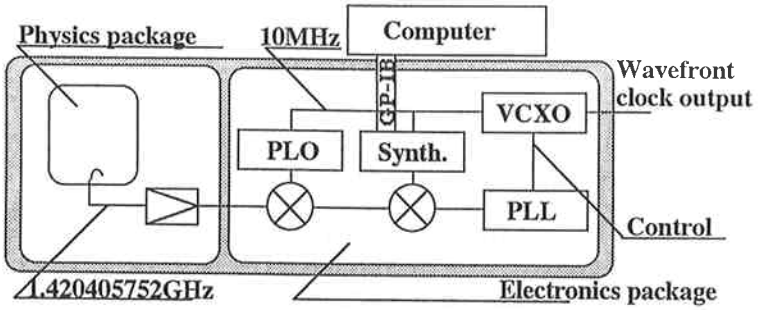

Fig. 12a Directly controlled wavefront clock.

4.1.2 A general use wavefront clock

As mentioned above, the output of a hydrogen maser is a fixed frequency. In this type of wavefront clock system, however, it is not necessary to improve the electronics of the hydrogen maser. This wavefront clock system is established between the hydrogen maser and the VLBI system, as shown in Fig. 12b. The source of the frequency oscillator is a BVA crystal oscillator, which has high signal clarity and can be used as a VLBI signal reference[14]. In this system, the BVA crystal is used as VCXO, which is phase-locked to the hydrogen maser. In order to obtain high frequency resolution, the reference signal from the hydrogen maser is multiplied by PLO (phase-locked oscillator). The frequency of the PLO is selected as 1.400 GHz. An a priori frequency value is calculated by a priori calculation software, as described in Subsection 4.2. The VCXO is controlled by a PLL circuit and the output frequency depends on the synthesizer frequency, which is under control of the host computer. Since the frequency variable range of a BVA crystal is 4×10^{-8}, another circuit must be provided for the high fringe rate ($>4 \times 10^{-8}$) in for example international VLBI experiments. This circuit is realized by a dual frequency synthesizer, whose phase is phase-locked to the BVA crystal oscillator. Fringe rotation and delay rate between two stations' data are frozen when the wavefront clock system is started. At correlation processing, only the delay bits at the observation start time are provided by the host computer. This bit shift is performed in buffer memory in the correlation processor. A fringe

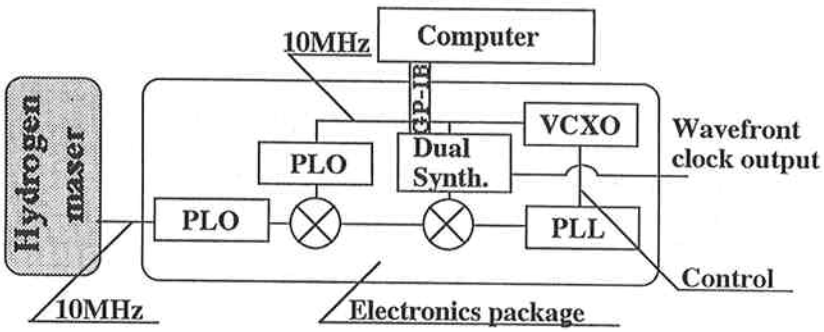

Fig. 12b General use wavefront clock.